Bioorganic Chemistry 100 (2020) 103967

Contents lists available at ScienceDirect

Bioorganic Chemistry

journal homepage: www.elsevier.com/locate/bioorg

Structural optimization of imidazothiazole derivatives affords a new promising series as B-Raf V600E inhibitors; synthesis, *in vitro* assay and *in silico* screening

Usama M. Ammar[a,b,c], Mohammed S. Abdel-Maksoud[d], Eslam M.H. Ali[a,b], Karim I. Mersal[a,b], Kyung Ho Yoo[e], Chang-Hyun Oh[a,b,*]

[a] Center for Biomaterials, Korea Institute of Science & Technology (KIST School), Seoul, Seongbuk-gu 02792, Republic of Korea
[b] University of Science & Technology (UST), Daejeon, Yuseong-gu 34113, Republic of Korea
[c] Pharmaceutical Chemistry Department, Faculty of Pharmacy, Ahram Canadian University, Giza 12566, Egypt
[d] Medicinal & Pharmaceutical Chemistry Department, Pharmaceutical and Drug Industries Research Division, National Research Centre (NRC), Dokki, Giza 12622, Egypt
[e] Chemical Kinomics Research Center, Korea Institute of Science and Technology, Seoul, Republic of Korea

ARTICLE INFO

Keywords:
Anti-cancer
B-Raf V600E
Cancer
Imidazo[2,1-*b*]thiazole
In silico screening

ABSTRACT

BRAF mutation is commonly known in a number of human cancer types. It is counted as a potential component in treating cancer. In this study, based on structural optimization of previously reported inhibitors (3-fluro substituted derivatives of imidazo[2,1-*b*]thiazole-based scaffold), we designed and synthesized sixteen new imidazo[2,1-*b*]thiazole derivatives with *m*-nitrophenyl group at position 6. The electron withdrawing properties was reserved while the polarity was modified compared to previously synthesized compounds (-F). Furthermore, the new substituted group (–NO_2) provided an additional H-bond acceptor(s) which may bind with the target enzyme through additional interaction(s). *In vitro* cytotoxicity evaluation was performed against human cancer cell line (A375). In addition, *in vitro* enzyme assay was performed against mutated B-Raf (B-Raf V600E). Compounds **13a, 13g** and **13f** showed highest activity on mutated B-Raf with IC_{50} 0.021, 0.035 and 0.020 μM. All target compounds were tested for *in vitro* cytotoxicity against NCI 60 cell lines. Compounds **13a** and **13g** were selected for 5 doses test mode. Moreover, *in silico* molecular simulation was explored in order to explore the possible interactions between the designed compounds and the B-Raf V600E active site.

1. Introduction

Cancer remains the main cause of high mortality rate in the globe after cardiac diseases [1–4]. It claims > 6 million human death per a year and still growing based on the WHO records [1]. Around 200 cancers were reported in different vital organs in human body [1]. Recent genetic screening showed that malignant tumors display a huge molecular events which can be used as a significant and potential therapeutic target for the treatment of cancer [5–12]. Mutation in BRAF have been reported as the major component in a number of human cancer types such as melanoma, thyroid and colon cancer [5,11,13–15]. This component is considered an important key in the MAPK pathway and play a major role in its the activation [5,15–17]. Mutation in BRAF occurs due to a single glutamate substitution for valine amino acid at position 600 (BRAF V600E) [5]. A number of drugs have been reported as mutated B-Raf inhibitors such as sorafenib (**I**) [18], vemurafenib(**II**) [19,20], dabrafenib(**III**) [21] and encorafenib(**IV**) [22,23] (Fig. 1). Although a diversity of anti-cancer agents have been developed, it is essential to enhance the anti-cancer properties of the existing drugs and discovery of new candidates for specific types of human cancer [1,24]. Heteroatoms-bearing molecules are considered a substantial structural motifs for drug development as they exhibit additional connectivity with the target biological receptor through H-bonding interaction [25–27]. The bi- and tri-cyclic fused heterocyclic rings show a significant platform for a wide range of anti-cancer agents [27,28]. Among these heterocyclic scaffolds, imidazothiazole is becoming an interesting molecular scaffold in pharmaceutical chemistry field due to its broad spectrum pharmacological properties. We previously reported the synthesis of imidazothiazole derivatives with B-Raf V600E inhibitory activity [29]. In the present work, structural optimization of imidazothiazole derivatives has been considered to afford a new series of NO_2-bearing compounds in which the fluoro group of previously

* Corresponding author at: Center for Biomaterials, Korea Institute of Science & Technology (KIST School), Seoul, Seongbuk-gu 02792, Republic of Korea.
E-mail address: choh@kist.re.kr (C.-H. Oh).

https://doi.org/10.1016/j.bioorg.2020.103967
Received 10 February 2020; Received in revised form 13 May 2020; Accepted 20 May 2020
Available online 22 May 2020
0045-2068/

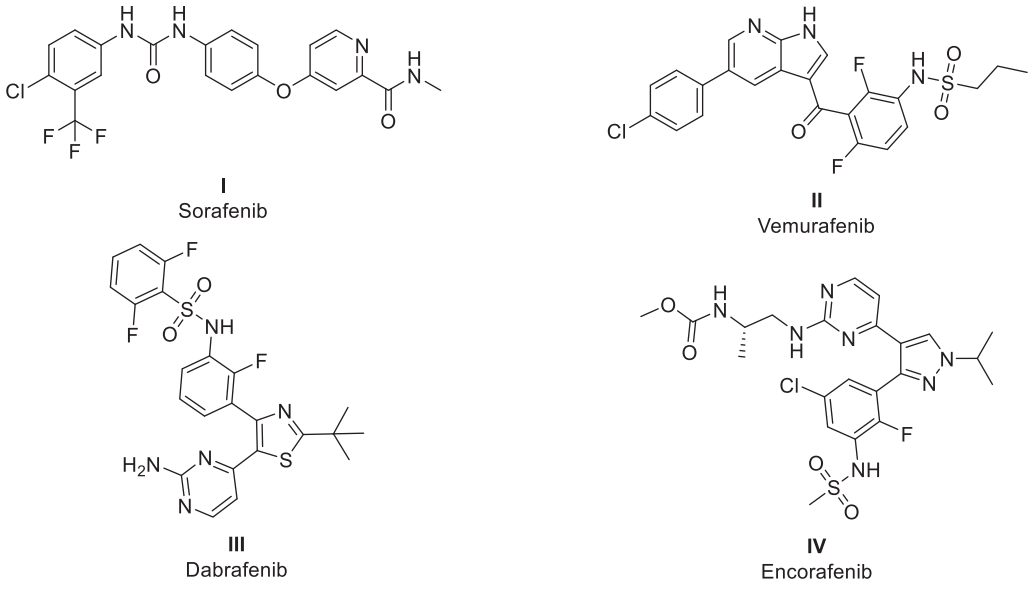

Fig. 1. Reported B-Raf V600E inhibitors.

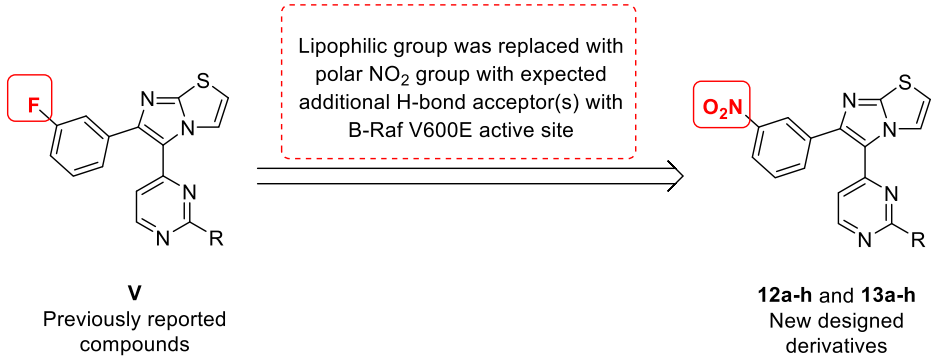

Fig. 2. The rational design of new synthesized derivatives (**12a-h** and **13a-h**).

reported compounds **V** (Fig. 2)[29] was replaced with NO_2 group. The electron withdrawing property was reserved while additional H-bond acceptor(s) were incorporated in the designed derivatives which may increase the binding to the B-Raf V600E active site.

2. Results and discussion

2.1. Chemistry

Final compounds **12a-h** and **13a-h** were synthesized as depicted in Scheme 1. *N*-based side chain (**3a-h** and **4a-h**) were prepared through nucleophilic substitution reaction between diamines (**1a,b**) and different substituted benzene sulfonyl chlorides (**2a-h**) [30]. α-bromination of 3′-nitroacetophenone (**5**) have been accomplished using *N*-bromosuccinamide in DMF to give compound **6**. ^{1}H NMR spectrum showed a singlet downfield signal at 5.06 ppm assigned for CH_2Br. Condensation of compound **6** with 2-aminothiazole (**7**) in MeOH provided compound **8**. ^{1}H NMR exhibited an additional signals at aromatic range at δ 8.25, 8.09 and 7.32 ppm attributed to the imidazothiazole protons. Moreover, disappearance of CH_2Br protons signals at δ 5.06 ppm. Coupling of compound **8** with compound **9** is accomplished through carbon–carbon bond- forming reaction (Heck reaction) [4,31] in presence of a catalytic amount of palladium acetate, Ph_3P and K_2CO_3 to provide compound **10**. ^{1}H NMR showed an additional aromatic protons signals at δ 6.86 and 7.06 ppm attributed the pyrimidine ring. Furthermore, additional signals at δ 2.67 ppm contributed to the SCH_3 protons. In addition, ^{13}C NMR showed an additional signal at aliphatic range at δ 14.23 ppm. Oxidation of SCH_3 of compound **10** was accomplished by reaction with potassium peroxymonosulfate to afford the key intermediate (**11**). ^{1}H NMR showed downfield-shift signal at δ 3.42 ppm attributed to SO_2CH_3 protons. Moreover, ^{13}C NMR showed downfield-shift signal at δ 39.28 ppm. Final target compounds **12a-h** and **13a-h** (Table 1) were provided by reaction between intermediate (**11**) and different appropriate *N*-based side chain (**3a-h** and **4a-h**) in presence of base. ^{1}H NMR showed an additional signals in both aromatic and aliphatic ranges attributed to the protons of built side chain.

2.2. Biological evaluation

2.2.1. In vitro enzyme assay

All synthesized compounds were tested against mutated B-Raf (B-Raf V600E). Final compounds were tested for both % inhibition at 10 μM (Table 2) and in 10-dose IC_{50} with a 3-fold serial dilution at 1 μM (Table 3). The assays were carried out at 1 μM ATP. In general, all new compounds showed higher activity to B-Raf V600E compared to wild-type B-Raf. Compounds 12e and 13f completely inhibited the mutated enzyme at the tested concentration.

The results showed that all compounds showed sub-micromolar IC_{50s}. Compounds **12e**, **13a, 13 g** and **13f** showed higher inhibitory activities among the synthesized compounds (0.027, 0.021, 0.035 and 0.020 μM, respectively). Compounds **12b, 12 g, 13c** and **13e** had higher IC_{50s} with values 0.072, 0.096, 0.082 and 0.063 μM. Finally, compounds **12a, 12c, 12d, 12f, 13b**, and **13d** exhibited moderate inhibitory effect with IC_{50} 0.158, 0.297, 0.103, 0.148, 0.216, and

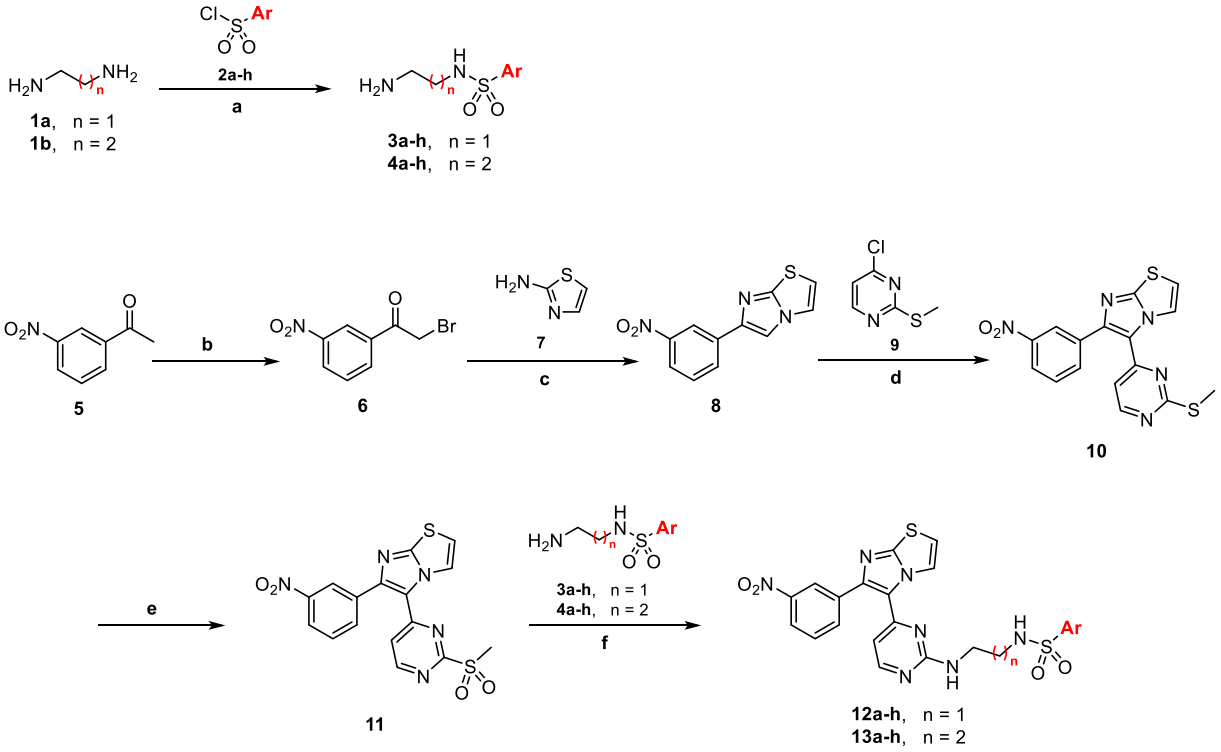

Scheme 1. Reagents and conditions. **a)** TEA, DCM, 0 °C-rt, 8 h; **b)** NBS, DMF, 60 °C, 3 h; **c)** MeOH, reflux, 18 h; **d)** $Pd(OAc)_2$, Ph_3P, K_2CO_3, DMF, 80 °C, 8 h; **e)** Oxone, $MeOH/H_2O$, rt, 9 h; **f)** DIPEA, DMSO, 90 °C, 8 h.

Table 1
Key structure of target compounds **12a-h** and **13a-h**.

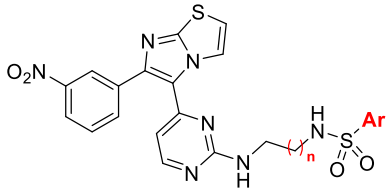

Target compounds

Compd	n	Ar	Compd	n	Ar
12a	1	3-FPh	**13a**	2	3-FPh
12b	1	4-CH_3Ph	**13b**	2	4-CH_3Ph
12c	1	4-CF_3Ph	**13c**	2	4-CF_3Ph
12d	1	4-OCH_3Ph	**13d**	2	4-OCH_3Ph
12e	1	4-ClPh	**13e**	2	4-ClPh
12f	1	4-BrPh	**13f**	2	4-BrPh
12 g	1	4-FPh	**13 g**	2	4-FPh
12 h	1	1-Naph	**13 h**	2	1-Naph

Table 3
IC_{50} values (μM) of target compounds (**12a-h** and **13a-h**) against B-Raf V600E.

Compd	B-Raf V600E IC_{50} (μM)	Compd	B-Raf V600E IC_{50} (μM)
12a	0.158 ± 0.0011	**13a**	0.021 ± 0.0007
12b	0.096 ± 0.0009	**13b**	0.216 ± 0.0016
12c	0.297 ± 0.0013	**13c**	0.082 ± 0.0015
12d	0.103 ± 0.0021	**13d**	0.131 ± 0.0021
12e	0.027 ± 0.0014	**13e**	0.063 ± 0.0006
12f	0.148 ± 0.0008	**13f**	0.020 ± 0.0003
12 g	0.072 ± 0.0012	**13 g**	0.035 ± 0.0021
12 h	0.634 ± 0.0021	**13 h**	0.259 ± 0.0019
Vemurafenib	0.031		

0.131 μM. Compounds **12e**, **13a** and **13f** had IC_{50s} lower than vemurafenib

The structure activity relationship for ethylene bridged compounds 12a-h revealed that moderate size electron-withdrawing group such as Cl **12e** had the highest activity over the mutated enzyme followed by small size electron-withdrawing group such as F in **12 g**. Compound that had small size electron donating group such as methyl in **12b** gave an 2 digits nano-molar IC_{50} . large size electron withdrawing group like

Table 2
Mean % inhibition of target compounds (**12a-h** and **13a-h**) against B-Raf V600E and wild-type B-Raf.

Compd	B-Raf V600E	B-Raf (WT)	Compd	B-Raf V600E	B-Raf (WT)
12a	96.72 ± 0.12	64.12 ± 1.23	**13a**	99.64 ± 0.22	66.31 ± 1.36
12b	98.62 ± 0.22	71.52 ± 0.99	**13b**	97.26 ± 0.16	69.36 ± 2.22
12c	95.87 ± 0.21	78.25 ± 1.11	**13c**	98.32 ± 0.24	71.66 ± 0.97
12d	96.99 ± 0.34	72.63 ± 1.35	**13d**	96.88 ± 0.17	70.35 ± 0.55
12e	100	76.14 ± 0.81	**13e**	98.97 ± 0.33	77.91 ± 1.65
12f	97.52 ± 0.41	72.51 ± 0.98	**13f**	100	75.16 ± 1.19
12 g	99.14 ± 0.19	70.25 ± 0.96	**13 g**	95.21 ± 0.31	69.26 ± 1.09
12 h	94.68 ± 0.11	59.81 ± 0.86	**13 h**	96.45 ± 0.28	65.33 ± 2.01

Fig. 3. Mean % inhibition of final target compounds against different cancer sub-types.

triflouromethyl and bromo derivatives **12c** and **12f** were less active compared to small size electron with-drawing group but more active compared to large planer naphthyl derivative **12 h**. On the other hand, compounds with propylene bridge **13a-h** showed less IC_{50} in general compared to ethylene analogues. Compound with large electron with drawing bromine atom**13f** had the highest activity in this group followed by unsubstituted benzene ring **13a** and small electron with drawing substituted derivative **12 g.** In similar manner to ethylene compounds, large aryl group such as naphthyl ring **13 h** had the lowest activity in this group.

2.2.2. In vitro cytotoxicity

2.2.2.1. NCI-60 human cell lines

2.2.2.1.1. One-dose 60 cell line assay. All final derivatives were accepted by the National Cancer Institute (NCI), and selected for one-dose 60 human cancer cell line assay (breast, colon, leukemia, melanoma, non-small cell lung, ovarian, prostate and renal cancer). All derivatives exhibited broad spectrum cytotoxic inhibitory effect against all NCI human cancer cell lines (Fig. 3 and Table 2**s**).

In general, compounds **13a** and **13 g** showed the highest % inhibition against nine cancer sub-types. **13a** and **13 g** showed 100% inhibition for melanoma cell lines and 90% inhibition against leukemia and prostate cancer. In addition, both compounds inhibited colon cancer, NSCLC, ovarian cancer and breast cancer with % inhibition of 80%.

The in deep results study showed that all compounds had different % inhibition against NCI-60 human cancer cell lines. Compounds **12c**, **13b-d** and **13f** showed moderate mean % inhibition against all cancer cell lines. Compounds **13a** and **13 g** showed potent % inhibition against NCI cancer cell lines. Compounds with propyl spacer showed higher inhibitory activities than that of ethyl spacer.

Regarding breast cancer (Table 2**s**), compounds **13 g** and **13a** exhibited 100% against BT-549, MCF7, MDA-MB-468 and T-47D cell lines. Compounds **13f**, **13d** and **13e** had % inhibition 98.2, 96.69, and 93.45 against T-47D cell line and 70.77, 83.80 and 86.87% against MDA-MB-468. Compounds **12f** and **12 g** showed their highest effect against T-47D with % inhibition 85.31 and 88, respectively.

On the other hand, the activity of the new compounds against CNS cancer cell lines (Table 3**s**) was moderate to low with highest % inhibition 94.43% for **13 g** against SF-295 cell line followed by **13a** with 94.14% against the same cell line.

The activity of the new series against colon cancer cell lines was presented at Table 4**s**. Compound **13a** completely inhibited the growth of HCT-15 and KM12 and inhibited COLO 205 by 95.48% and HCT-116 with % inhibition 95.57% and SW-620 with 81.68%. While **13a** inhibited COLO205 and KM12 completely at 10 μM. Also **13a** inhibited HCT-116, and HCT-15 with mean % inhibition 92.23 and 97.79, respectively. Compounds **13c**, **13d**, **13e**, and **13f** showed > 50% inhibition against COLO205, HCT-16, HT29 and KM12 cell lines.

Compounds **13a** and **13 g** were able to cease the growth of HL-60, MOLT-4 and RPMI-8226 cell lines. Compound **12b** showed > 50% inhibition against CCRF-CEM, K562, MOLT-4 and RPMI-8226. While compound **12c** had > 50% inhibition against all leukemia cell lines. Compounds **13b, 13c, 13d, 13e**, and **13f** with propyl bridge between pyrimidine ring and terminal sulfonamide moiety showed higher % inhibition against the leukemia cell lines compared to their ethyl analogues (Table 5**s**).

Compounds **13a** and **13 g** inhibited all melanoma cell lines at tested dose. In addition, compounds **13c**, **13d**, **13e** and **13f** successfully inhibited LOX IMVI, M14, MDA-MB-435, SK-MEL-2, and UACC-62 cell lines with % inhibition of 50%.

In addition to the above mentioned cell lines, compounds **13a** and **13 g** completely inhibited NCI-H226, NCI-H23 and NCI-H522 non-small cell lung cancer cell lines, NCI/ADRRES, OVCAR-3, OVCAR-4 and

Table 4
% inhibition of most potent compounds (**12a, 12c**, **13a and 13 g**) against NCI 60 cell lines at single dose (10 μM).

Cell line		12b	12c	13a	13g
Breast Cancer	BT-549	74.35	73.58	100.00	100.00
	HS 578 T	17.10	33.56	68.82	77.85
	MCF7	64.59	78.07	100.00	100.00
	MDA-MB-231/ ATCC	27.01	39.80	52.36	55.13
	MDA-MB-468	56.63	71.71	100.00	100.00
	T-47D	86.42	100.00	100.00	100.00
CNS cancer	SF-268	54.23	60.24	88.17	90.68
	SF-295	34.34	62.59	94.17	94.43
	SF-539	12.89	25.46	65.23	73.54
	SNB-19	24.26	38.59	58.80	70.67
	U251	29.94	48.61	60.22	73.22
Colon cancer	COLO 205	42.12	62.80	100.00	95.48
	HCC-2998	ND	34.80	34.40	41.70
	HCT-116	42.91	64.36	92.23	95.57
	HCT-15	50.49	73.27	97.79	100.00
	HT29	59.30	60.01	78.66	81.56
	KM12	81.11	77.49	100.00	99.01
	SW-620	ND	30.18	77.13	81.68
Leukemia	CCRF-CEM	63.04	79.75	96.96	98.05
	HL-60(TB)	36.30	84.00	100.00	100.00
	K-562	58.59	78.15	95.74	92.49
	MOLT-4	62.24	81.85	100.00	100.00
	RPMI-8226	63.72	95.20	100.00	100.00
	SR	49.47	60.81	86.78	90.99
Melanoma	LOX IMVI	46.03	69.58	100.00	100.00
	M14	39.08	62.22	100.00	99.98
	MALME-3 M	10.83	58.89	100.00	100.00
	MDA-MB-435	56.29	79.28	100.00	98.34
	SK-MEL-2	39.52	73.10	100.00	100.00
	SK-MEL-28	7.02	41.20	100.00	100.00
	SK-MEL-5	81.90	100.00	100.00	100.00
	UACC-257	29.58	50.88	100.00	99.98
	UACC-62	53.68	86.79	100.00	100.00
Non-small cell lung cancer	A549/ATCC	53.94	68.11	92.73	90.33
	EKVX	34.58	60.48	80.89	81.75
	HOP-62	9.57	26.98	86.94	87.54
	HOP-92	36.78	55.26	53.67	53.77
	NCI-H226	46.07	59.70	100.00	100.00
	NCI-H23	23.39	56.74	100.00	100.00
	NCI-H322M	30.81	38.20	54.79	73.24
	NCI-H460	39.96	66.63	83.66	89.55
	NCI-H522	40.57	65.73	100.00	99.88
Ovarian cancer	IGROV1	54.63	72.86	96.82	94.97
	NCI/ADR-RES	51.53	73.09	100.00	100.00
	OVCAR-3	41.68	59.46	100.00	95.88
	OVCAR-4	64.60	68.76	100.00	100.00
	OVCAR-5	ND	12.64	33.80	40.87
	OVCAR-8	54.87	73.90	100.00	96.56
	SK-OV-3	3.42	26.04	55.35	62.88
Prostate cancer	DU-145	49.90	51.53	90.23	89.44
	PC-3	64.70	82.99	100.00	100.00
Renal cancer	786–0	36.21	39.66	56.58	55.79
	A498	45.75	63.41	66.29	70.29
	ACHN	59.56	77.54	93.64	94.62
	CAKI-1	50.20	69.75	89.99	90.21
	RXF 393	44.24	43.98	47.99	46.57
	SN12C	56.80	67.01	81.35	89.45
	TK-10	17.51	42.09	47.09	55.43
	UO-31	74.34	82.72	100.00	100.00

OVCAR-8 ovarian cancer cell lines, PC-3 prostate cancer cell line and UO-31 renal cancer cell line (Tables 4, 1s-10s)

2.2.2.1.2. Five-dose 60 cell line assay. Compounds **13a** and **13 g** (the most active compounds in one-dose assay) were selected by the NCI to be evaluated in five-dose assay in order to identify their GI_{50} values NCI human cancer cell lines (Table 5 and 6).

Compounds **13a** and **13g** showed mean GI_{50} of range 1.90 – 3.94 μM against all NCI human cancer cell lines. They exhibited potent mean GI_{50} against prostate cancer cell lines (mean GI_{50} 1.99 and 1.90 μM, respectively) and melanoma cell lines (mean GI_{50} 2.21 and

Table 5
GI_{50} and TGI values (μM) of compounds **13a** and **13 g** against NCI-60 cancer cell lines.

NCI-cell lines	GI_{50}		TGI	
	13a	13 g	13a	13g
Breast Cancer				
BT-549	2.18	2.14	11.90	7.03
HS 578 T	4.73	3.25	47.30	> 100
MCF7	2.16	2.53	8.48	ND
MDA-MB-231/ATCC	6.41	4.98	27.2	> 100
MDA-MB-468	0.83	1.50	6.10	7.11
T-47D	0.39	3.03	4.64	2.82
CNS Cancer				
SF-268	3.21	2.92	21.9	> 100
SF-295	2.52	2.62	7.79	8.15
SF-539	4.04	3.61	20.8	> 100
SNB-19	4.34	4.01	61.8	> 100
U251	4.56	3.73	39.40	> 100
Colon Cancer				
COLO 205	2.46	2.44	8.11	8.24
HCC-2998	6.79	7.29	> 100	> 100
HCT-116	2.74	2.85	> 100	> 100
HCT-15	2.30	2.08	12.30	9.79
HT29	3.12	2.90	> 100	> 100
KM12	2.39	2.59	8.14	7.91
SW-620	4.12	3.95	> 100	> 100
Leukemia				
CCRF-CEM	1.30	1.20	> 100	7.81
HL-60(TB)	2.97	2.55	8.57	6.69
K-562	1.73	1.62	> 100	> 100
MOLT-4	1.17	1.23	ND	5.52
RPMI-8226	9.84	0.68	4.18	2.94
SR	3.10	2.53	> 100	> 100
Melanoma				
LOX IMVI	2.58	2.57	11.00	1.04
M14	2.82	2.72	12.00	> 100
MALME-3 M	2.14	2.00	7.06	6.76
MDA-MB-435	2.98	2.55	11.6	7.93
SK-MEL-2	2.04	2.06	5.98	5.43
SK-MEL-28	2.63	2.75	7.76	7.92
SK-MEL-5	0.82	1.06	2.10	2.45
UACC-257	2.71	2.54	8.27	7.96
UACC-62	1.16	1.20	4.26	4.21
Non-Small Cell Lung Cancer				
A549/ATCC	2.68	2.73	24.30	> 100
EKVX	2.77	2.90	52.70	> 100
HOP-62	3.50	3.16	14.10	9.61
HOP-92	2.80	1.74	30.30	> 100
NCI-H226	1.66	1.95	8.22	7.60
NCI-H23	1.98	2.42	7.34	9.16
NCI-H322M	3.99	3.21	285	> 100
NCI-H460	3.34	2.94	> 100	> 100
NCI-H522	2.02	1.59	7.97	6.020
Ovarian Cancer				
IGROV1	2.71	2.90	11.60	26.8
NCI/ADR-RES	1.72	1.85	6.49	7.31
OVCAR-3	2.53	2.31	11.90	8.49
OVCAR-4	1.64	1.65	7.64	6.55
OVCAR-5	7.83	5.63	> 100	> 100
OVCAR-8	1.89	1.74	17.70	22.20
SK-OV-3	5.82	4.17	30.50	> 100
Prostate Cancer				
DU-145	2.60	2.65	12.90	12.90
PC-3	1.37	1.14	6.62	4.82
Renal Cancer				
786–0	7.97	7.39	45.60	> 100
A498	1.56	1.87	30.50	> 100
ACHN	2.19	2.19	11.20	10.80
CAKI-1	2.33	2.33	14.10	> 100
RXF 393	8.13	6.95	41.60	> 100
SN12C	2.71	2.61	44.70	> 100
TK-10	5.38	4.34	52.10	> 100
UO-31	1.25	1.40	9.04	8.39

Table 6
Mean GI_{50} and TGI of compounds **13a** and **13 g** against NCI-60 cancer cell lines.

NCI-cell lines	Mean GI_{50} (μM)		Mean TGI (μM)	
	13a	13g	13a	13g
Breast Cancer	2.78	2.91	17.60	5.65
CNS Cancer	3.73	3.38	30.34	8.15
Colon Cancer	3.42	3.44	9.52	8.65
Leukemia	3.35	1.64	6.38	5.74
Melanoma	2.21	2.16	7.78	5.46
Non-Small Cell Lung Cancer	2.75	2.52	53.74	8.10
Ovarian Cancer	3.45	2.89	14.31	14.27
Prostate Cancer	1.99	1.90	9.76	8.86
Renal Cancer	3.94	3.64	31.11	9.60

Table 7
Mean GI_{50} and TGI of compounds **13a** and **13 g** compared to different singling agents.

Compounds	Mean GI_{50} (μM)	Mean TGI (μM)
13a	3.07	20.06
13g	2.72	8.28
Dasatinib	0.33	8.9
Erlotinib	5.5	59
Gefitinib	3.2	19
Imatinib	15	43
Lapatinib	2.9	20
Nilotinib	2.9	13

Table 8
IC_{50} (μM) of target compounds **13a-h**, vemurafenib and sorafenib against human melanoma cell line (A375).

Compd	A375 IC_{50} (μM)	Compd	A375 IC_{50} (μM)
13a	2.99	**13f**	> 10
13b	4.51	**13g**	7.96
13c	7.87	**13h**	> 10
13d	> 10	**Sorafenib**	10.28
13e	10.68	**Vemurafenib**	5.9

2.16 μM, respectively). Moreover, compound **13 g** exhibited higher inhibitory activities against all NCI human cancer cell lines than that of **13a** (mean GI_{50} 2.72 and 3.07 μM, respectively). The results revealed that compounds with *para* substituted phenyl ring in side chain with F group (**13 g**) were more active that that with *meta* F (**13a**).

Compounds **13a** and **13 g** showed activities that are more potent compared to Erlotinib, Gefitinib and Imatinib [32] in term of mean GI_{50} over NCI 60 cell lines. Compound 13 g had lower GI_{50} compared to Erlotinib, Gefitinib, Imatinib, Lapatinib, Nilotinib but higher compared to Dasatinib. The total growth inhibition of **13 g** was lower compared to six singling agents while 13a was more potent than Erlotinib, and Imatinib.(see Table 7)

Table 9
IC_{50} (μM) of target compounds **12a-h** and**13a-h**, human embryonic pulmonary epithelial cells (L132).

Compd	L132 IC_{50} (μM)	Compd	L132 IC_{50} (μM)
12a	91	**13a**	80
12b	101	**13b**	95
12c	69	**13c**	70
12d	75	**13d**	77
12e	80	**13e**	88
12f	90	**13f**	82
12 g	82	**13 g**	76
12h	94	**13h**	86

2.2.2.2. In vitro assay against A375 melanoma cell line. Compounds **13a-h** were selected for testing their cytotoxic inhibitory activity against melanoma cell line (A375) (Table 8). Their activities were compared to both vemurafenib and sorafenib as standards using MTT (3-(4,5-dimethylthiazol-2-yl)-2,5-diphenyltetrazoliumbromide)assay [33].

The results revealed that NO_2-bearing derivatives showed different inhibitory activities against melanoma cell line (A375). In addition, most of compounds had comparable inhibitory activities to sorafenib (IC_{50} 10.28 μM). Furthermore, compounds **13a** and **13b** exhibited potent inhibitory activities (IC_{50} 2.99 and 4.51 μM, respectively) compared to sorafenib (IC_{50} 10.28 μM).

In addition to the ability of new target compounds to inhibit A375 proliferation, compounds 13a and 13 g were tested for their ability to inhibit phosphorylation of both MEK and ERK in A375 cells. Both compounds showed significant reduction in phosphorylation of both enzyme starting from 1uM concentration. Both compounds were incubated with A375 cells and phosphorylated MEK and ERK were investigated using western plot analysis at three different doses 1, 3 and 10 uM (Fig. 4) .

In order to check the effect of the newly synthesized compounds over normal cell line to determined they toxicity, all final target compounds were tested over human embryonic pulmonary epithelial cells (L132). The IC_{50s} over L132 cell line is presented in Table 9. All final target compounds showed at least 5 folds selectivity for cancer cell lines compared to normal cell line. For series **12a-h**, compounds **12b** had the highest IC_{50} with value 101 uM followed by **12 h** and **12a** with values 94 and 91uM. On the other hand, compound **13b** showed the highest IC_{50} with value 95 uM, followed by **13e, 13 h** and **13f** with IC_{50s} 88, 86 and 82 uM, respectively.

2.3. Molecular docking

The X-ray structural complex of PLX3203 (native ligand, PDB ID: 325) [34] with the B-Raf V600E protein (PDB ID: 4FK3) [33] was used in the molecular docking study of target compounds (**12a-h** and **13a-h**). The docking protocol used for the docking of native ligand was valid with virtual ligand screening (VLS) score of −6.6343 kcal/mol and route mean square deviation (RMSD) of 1.2458 (Fig. 5).

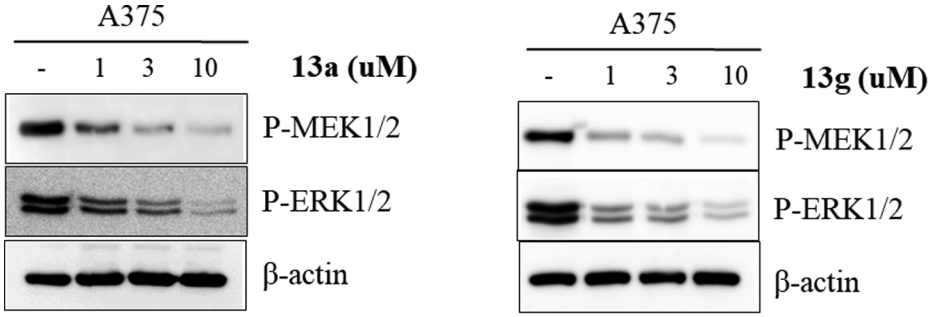

Fig. 4. The ability of compounds 13a and 13g to inhibit phosphorylation of ERK and MEK on A375 cell line.

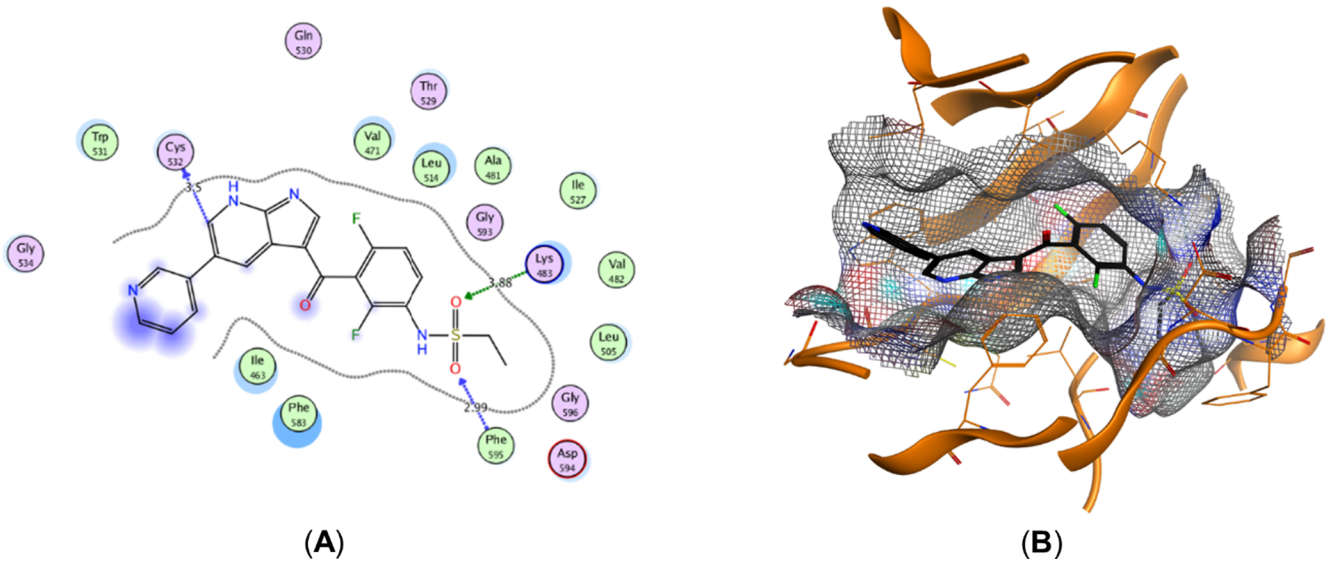

Fig. 5. 2D interaction (**A**) and 3D interaction (**B**) of native ligand (PLX2303) with B-Raf V600E (PDB ID: 4FK3) active site.

Most of target compounds (**12a-h** and **13a-h**) showed a number of interactions with the conserved amino acid residues of the active site (Val 471, Lys 483, Cys 532 and Asp 594). In addition, they exhibited VLS score range of −8.7141 to −6.2267 kcal/mol with different interactions (arene-cation and H bonding interactions) (Table 9**s**).

The results showed that most of synthesized compounds made additional interaction between substituted NO_2 and the amino acid residues in the active site of B-Raf V600E (Lys 483 and Asp 594). Moreover, compounds **12a**, **12d**, **13b** and **13g** exhibited higher binding scores with the active site among the synthesized derivatives (S = -8.3757, −8.7141, −8.0109 and −8.0237 kcal/mol, respectively) with 5 or 6 visible interactions (Fig. 6). Furthermore, these compounds (**12a**, **12d**, **13b** and **13 g**) showed additional H-bond interaction(s) through incorporated NO_2 group.

From the molecular docking studies, it was investigated that substituted NO_2 group has a significant effect in the binding mode with the B-Raf V600E active site through additional H-bond(s) with Lys 483 and 594.

3. Conclusion

A new series of imidazo[2,1-*b*]thiazole-based compounds derivatives was designed, synthesized and evaluated for their cytotoxic activity and enzyme assay. Compounds **13a** and **13 g** were the most active derivatives in cytotoxicity among the synthesized compounds. Compound **13a** showed potent *in vitro* enzyme inhibitory activity. Generally, compounds with halogenated substitution were more potent compared to other substitution or unsubstituted phenyl derivatives. Moreover, compounds with propyl linker between aryl sulfonamide terminal group and pyrimidine ring at position 5 of the imidazo[2,1-*b*] thiazole ring were more potent compared to that with ethyl linker. The molecular docking studies revealed that the incorporated NO_2 group in the terminal phenyl ring had a significant effect in the binding to the B-Raf V600E active site through additional H-bond interaction(s) with conserved amino acid residues. Finally, these results afforded NO_2-bearing imidazothiazole derivatives as a key scaffold for further molecular and structural optimization.

4. Experimental

All chemicals, including starting compounds, reagents and solvents, were obtained from Sigma-Aldrich Co., Tokyo Chemical Industry (TCI) Co. and Daejung Chemicals & Metals Co. and used without any purification. All reactions were monitored by TLC using Hexane/Ethyl acetate. All spots were visualized at 365 and 254 nm by Spectroline UV ENF-240C/FE (Spectronics Co., Westbury, New York, USA). All melting points were determined on Thomas-Hoover (Uni-Melt) Capillary Melting Point Apparatus (Arthur H. Thomas Company, Philadelphia PA., USA). The Nuclear Magnetic Resonance (NMR) were recorded on Bruker ARX-400, 400 MHz spectrometer (Bruker Bioscience, Billerica, MA, USA). Samples were prepared using deuterated Cambridge NMR solvents; $CDCl_3$, DMSO and MeOD. Chemical shift were quoted in ?? as parts per million (ppm) downfield from TMS as internal standard. Mass spectra (MS) were determined by LC-MS analysis using the following system: Water 2998 photodiode array detector, Water 3100 mass detector, Water SFO system fluidics organizer, Water 2545 binary gradient module, Water reagent manager, Waters 2767 sample manager, Sunfire™ C188 column (4.6 × 50 mm, 5 μm particle size); solvent gradient = 95% A at 0 min, 1% A at 5 min; solvent A = 0.04% trifluoroacetic acid (TFA) in water; solvent B = 0.04% TFA in MeOH; flow rate = 3.0 ml/min; AUC was calculated using Waters MassLynx 4.1 software.

4.1. Chemistry

4.1.1. General procedure for synthesis of N-(2-aminoethyl and 3-aminopropyl)unsubstituted and substituted phenyl sulfonamide (3a-h and 4a-h):

A solution of appropriate sulfonyl chloride (**2a-h**, 5 mmol) in dichloromethane (2 ml) was added dropwise to a solution of proper diamine (**1a,b**, 10 mmol) and trimethylamine (300 mg, 30 mmol) in dichloromethane (20 ml) at 0 °C. The reaction mixture was allowed to stir at rt for 18 h. The reaction mixture was washed with saturated solution of $NaHCO_3$ (20 ml). The organic layer was dried over anhydrous sodium sulfate and evaporated under vacuum to give the titled products **3a-h** and **4a-h** [30].

4.1.2. Synthesis of 2-bromo-1-(3-nitrophenyl)ethan-1-one (6):

N-bromosuccinamide (1.3 g, 7.2 mmol, 1.2 Eq) was added portionwise to a solution of compound **5** (1 g, 6 mmol, 1 Eq) in anhydrous DMF (5 ml) at rt. The reaction mixture was stirred at 60 °C for 3 h. The reaction mixture was cooled and extracted between EtOAc (40 ml) and water (60 ml). The organic layer was washed with water (3 × 50 ml). The organic layer was dried over anhydrous Na_2SO_4 and evaporated under vacuum. The crude residue was purified through column chromatography (hexane, EtOAc; 100, 1) to give the titled product **6**. Yield:

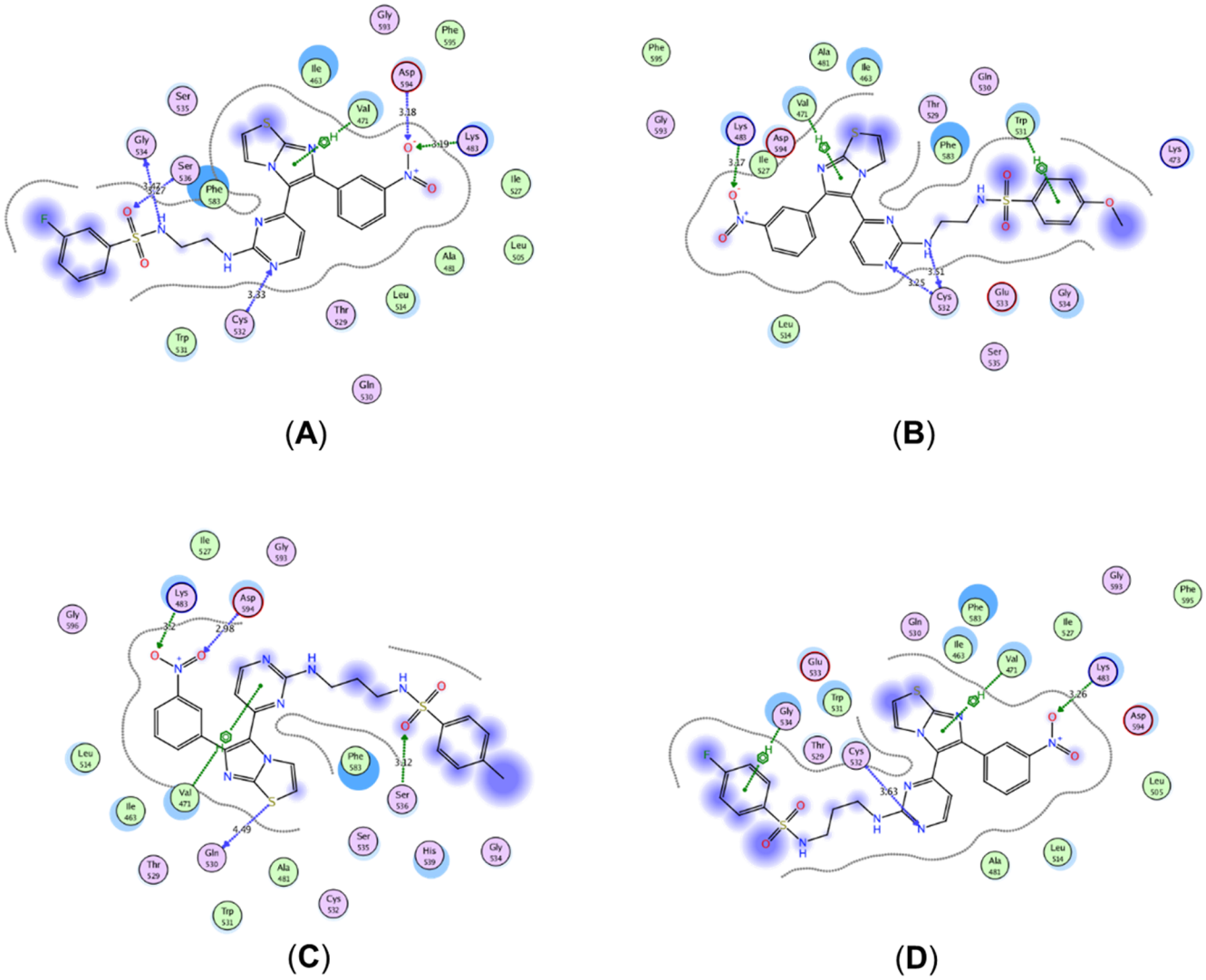

Fig. 6. 2D interaction of compounds **12a** (**A**), **12d** (**B**), **13b** (**C**) and **13g** (**D**) with B-Raf V600E (PDB ID: 4FK3) active site.

75%. m.p.: 95–6 °C. ^{1}H NMR (400 MHz, DMSO-d_6) δ 8.71 (t, J = 2.0 Hz, 1H, Ar-H), 8.51–8.48 (m, 1H, Ar-H), 8.44–8.41 (m, 1H, Ar-H), 7.87 (t, J = 8.0 Hz, 1H, Ar-H), 5.06 (s, 1H, CH_2Br). ^{13}C NMR (100 MHz, DMSO-d_6) δ 190.75 (Ar-C), 148.46 (Ar-C), 135.67 (Ar-C), 135.33 (Ar-C), 131.13 (Ar-C), 128.37 (Ar-C), 123.46 (Ar-C), 34.61 (CH2Br). LC/MS: 245 (M + 1)$^+$.

4.1.3. Synthesis of 6-(3-nitrophenyl)imidazo[2,1-b]thiazole (8):

A solution of compound **6** (1 g, 4.1 mmol, 1 Eq) and compound **7** (0.5 g, 4.9 mmol, 1.2 Eq) in MeOH (50 ml) was stirred under reflux for 18 h. The organic solvent was evaporated under vacuum. The crude solid ppt was stirred in NH_4OH solution at rt for 2 h. The crude solid product was filtered and washed with cold water (3 × 100 ml) and dried to give the titled product **8**. Yield: 90%. m.p.: 167–9 °C. ^{1}H NMR (400 MHz, DMSO-d_6) δ 8.63 (t, J = 2.2 Hz, 1H, Ar-H), 8.46 (s, 1H, Ar-H), 8.27–8.24 (m, 1H, Ar-H), 8.09–8.06 (m, 1H, Ar-H), 7.98 (d, J = 4.4 Hz, 1H, Ar-H), 7.67 (t, J = 8.2 Hz, 1H, Ar-H), 7.32 (d, J = 4.4 Hz, 1H, Ar-H). ^{13}C NMR (100 MHz, DMSO-d_6) δ 150.25 (Ar-C), 148.78 (Ar-C), 144.40 (Ar-C), 136.46 (Ar-C), 131.26 (Ar-C), 130.61 (Ar-C), 121.87 (Ar-C), 120.52 (Ar-C), 119.32 (Ar-C), 114.39 (Ar-C), 111.44 (Ar-C). LC/MS 246 (M + 1)$^+$.

4.1.4. Synthesis of 5-(2-(methylthio)pyrimidin-4-yl)-6-(3-nitrophenyl) imidazo[2,1-b]thiazole (10):

A solution compound **9** (0.7 g, 4.1 mmol, 1 Eq) in anhydrous DMF (5 ml) was added dropwise to a mixture of compound **8** (1 g, 4.1 mmol, 1 Eq), Ph_3P (0.3 g, 1.3 mmol, 0.3 Eq), K_2CO_3 (0.6 g, 4.1 mmol, 1 Eq) and $Pd(OAc)_2$ (0.2 g, 0.8 mmol, 0.2 Eq) in anhydrous DMF (10 ml). The reaction mixture was stirred at 80 °C for 8 h. The reaction mixture was cooled and stirred with crushed ice (30 g). The crude ppt was filtered. The crude solid residue was stirred in MeOH (50 ml) at 60 °C for 1 h. The solid product was filtered and washed with MeOH (3 × 20 ml) and dried to give the titled product **10**. Yield: 30%. m.p.: 187–9 °C. ^{1}H NMR (400 MHz, $CDCl_3$) δ 8.58 (d, J = 4.4 Hz, 2H, Ar-H), 8.34–8.31 (m, 2H, Ar-H), 8.02 (d, J = 8.0 Hz, 1H, Ar-H), 7.66 (t, J = 8.0 Hz, 1H, Ar-H), 7.06 (d, J = 4.4 Hz, 1H, Ar-H), 6.86 (d, J = 5.6 Hz, 1H, Ar-H), 2.66 (s, 3H, SCH_3). ^{13}C NMR (100 MHz, $CDCl_3$) δ 173.15 (Ar-C), 156.83 (Ar-C), 155.66 (Ar-C), 153.01 (Ar-C), 148.57 (Ar-C), 147.65 (Ar-C), 136.32 (Ar-C), 135.04 (Ar-C), 129.83 (Ar-C), 124.14 (Ar-C), 123.53 (Ar-C), 121.96 (Ar-C), 120.82 (Ar-C), 113.65 (Ar-C), 112.00 (Ar-C), 14.23 (SCH_3). LC/MS 371 (M + 1)$^+$.

4.1.5. Synthesis of 5-(2-(methylsulfonyl)pyrimidin-4-yl)-6-(3-nitrophenyl) imidazo[2,1-b]thiazole (11):

A solution of potassium peroxymonosulfate (5 g, 8.1 mmol, 3 Eq) in

water (20 ml) was added dropwise to a solution of compound **10** (1 g, 2.7 mmol, 1 Eq) in MeOH (50 ml). The reaction mixture was stirred at rt for 9 h. The organic solvent was evaporated under vacuum. The crude residue was extracted between DCM (70 ml) and water (30 ml). The organic layer was washed with brine solution (3 × 30 ml). The organic layer was dried over anhydrous Na_2SO_4 and evaporated under reduced pressure. The crude solid residue was purified through column chromatography (hexane, EtOAc; 2, 1) to give the titled product **11**. Yield: 80%. m.p.: 215–6 °C. ^{1}H NMR (400 MHz, $CDCl_3$) δ 8.91 (d, J = 4.4 Hz, 1H, Ar-H), 8.61 (t, J = 5.6 Hz, 2H, Ar-H), 8.39–8.37 (m, 1H, Ar-H), 8.04 (d, J = 8.0 Hz, 1H, Ar-H), 7.75 (t, J = 7.6 Hz, 1H, Ar-H), 7.35 (d, J = 5.6 Hz, 1H, Ar-H), 7.17 (d, J = 4.8 Hz, 1H, Ar-H), 3.42 (s, 3H, SO_2CH_3). ^{13}C NMR (100 MHz, $CDCl_3$) δ 166.13 (Ar-C), 157.49 (Ar-C), 154.59 (Ar-C), 149.59 (Ar-C), 148.70 (Ar-C), 135.71 (Ar-C), 130.32 (Ar-C), 124.21 (Ar-C), 123.16 (Ar-C), 120.01 (Ar-C), 117.48 (Ar-C), 114.79 (Ar-C), 39.27 (SO_2CH_3). LC/MS 403 $(M + 1)^+$.

4.1.6. General procedure for synthesis of N-substituted-4-(6-(3-nitrophenyl)imidazo[2,1-b]thiazol-5-yl)pyrimidin-2-amine (12a-h and 13a-h):

A mixture of compound **11** (0.2 g, 0.5 mmol, 1 Eq), appropriate amine (**3a-h** and **4a-h**, 0.6 mmol, 1.2 Eq) and *N*,*N*-diisopropylethylamine (0.6 g, 1.3 ml, 4.5 mmol, 9 Eq) in anhydrous DMSO (2 ml). The reaction mixture was stirred at 90 °C for 9 h. The reaction mixture was cooled and extracted between EtOAc (10 ml) and water (30 ml). The organic layer was washed with water (3 × 30 ml). The organic layer was dried over anhydrous Na_2SO_4 and evaporated under reduced pressure. The crude residue was purified through column chromatography (hexane, EtOAc; 1, 1) to give the titled product **12a-h** and **13 a-h**, respectively.

*4.1.6.1. 3-Fluoro-N-(2-((4-(6-(3-nitrophenyl)imidazo[2,1-b]thiazol-5-yl) pyrimidin-2-yl)amino)ethyl)benzenesulfonamide (**12a**):*. Yield: 60%. m.p.: 161–3 °C. ^{1}H NMR (400 MHz, DMSO-d_6) δ 8.44 (s, 1H, Ar-H), 8.28 (d, J = 8.0 Hz, 1H, Ar-H), 8.13 (d, J = 5.2 Hz, 1H, Ar-H), 8.08 (d, J = 4.0 Hz, 1H, Ar-H), 7.93 (s, 1H, NH), 7.78 (s, 1H, Ar-H), 7.56–7.65 (m, 4H, Ar-H), 7.48–7.55 (m, 3H, Ar-H), 3.41 (s, 2H, Aliph-H), 3.02 (t, J = 4.0 Hz, 2H, Aliph-H). ^{13}C NMR (100 MHz, DMSO-d_6) δ 163.44 (Ar-C), 160.98 (Ar-C), 148.38 (Ar-C), 143.04 (Ar-C), 136.64 (Ar-C), 135.76 (Ar-C), 132.08 (Ar-C), 130.69 (Ar-C), 123.51 (Ar-C), 123.17 (Ar-C), 120.27 (Ar-C), 120.09 (Ar-C), 119.88 (Ar-C), 114.08 (Ar-C), 113.84 (Ar-C), 42.65 (Aliph-C), 42.37 (Aliph-C). LC/MS 541 $(M + 1)^+$.

*4.1.6.2. 4-Methyl-N-(2-((4-(6-(3-nitrophenyl)imidazo[2,1-b]thiazol-5-yl) pyrimidin-2-yl)amino)ethyl)benzenesulfonamide (**12b**):*. Yield: 80%. m.p.: 98–100 °C. ^{1}H NMR (400 MHz, DMSO-d_6) δ 8.44 (t, J = 1.6 Hz, 1H, Ar-H), 8.28 (d, J = 7.6 Hz, 1H, Ar-H), 8.13 (d, J = 4.8 Hz, 1H, Ar-H), 8.08 (d, J = 7.6 Hz, 1H, Ar-H), 7.78 (s, 1H, Ar-H), 7.68 (d, J = 8.4 Hz, 3H, Ar-H), 7.62 (d, J = 8.4 Hz, 1H, Ar-H), 7.52 (s, 1H, NH), 7.34–7.43 (m, 3H, Ar-H), 6.42 (s, 1H, NH), 3.40 (s, 2H, Aliph-H), 2.95 (d, J = 6.0 Hz, 2H, Aliph-H), S.34 (s, 3H, CH_3). ^{13}C NMR (100 MHz, DMSO-d_6) δ 149.39 (Ar-C), 143.18 (Ar-C), 143.09 (Ar-C), 137.89 (Ar-C), 137.83 (Ar-C), 136.66 (Ar-C), 135.77 (Ar-C), 130.69 (Ar-C), 130.11 (Ar-C), 130.04 (Ar-C),126.95 (Ar-C), 124.93 (Ar-C), 124.91(Ar-C), 123.74 (Ar-C), 124.52 (Ar-C), 42.6 (Aliph-C), 42.37 (Aliph-C), 21.4 (CH_3). LC/MS 537 $(M + 1)^+$.

*4.1.6.3. N-(2-((4-(6-(3-Nitrophenyl)imidazo[2,1-b]thiazol-5-yl) pyrimidin-2-yl)amino)ethyl)-4-(trifluoromethyl)benzenesulfonamide (**12c**):*. Yield: 85%. m.p.: 145–7 °C. ^{1}H NMR (400 MHz, DMSO-d_6) δ 8.44 (s, 1H, Ar-H), 8.28 (d, J = 7.6 Hz, 1H, Ar-H), 8.13 (s, 2H, Ar-H), 8.08 (d, J = 6.4 Hz, 3H, Ar-H), 8.01 (d, J = 8.0 Hz, 1H, Ar-H), 7.83 (t, J = 8.4 Hz, 1H, Ar-H), 7.76 (t, J = 8.0 Hz, 1H, Ar-H), 7.51 (s, 1H, Ar-H), 6.43 (s, 1H, Ar-H), 3.41 (s, 2H, Aliph-H), 3.03 (t, J = 6.4 Hz, 2H, Aliph-H). ^{13}C NMR (100 MHz, DMSO-d_6) δ 162.32 (Ar-C),148.38 (Ar-C), 142.16 (Ar-C), 136.64 (Ar-C), 135.75 (Ar-C), 131.31 (Ar-C), 131.64 (Ar-C), 130.68 (Ar-C), 130.47 (Ar-C), 130.15 (Ar-C), 129.58 (Ar-C), 125.25 (CF3), 123.78 (Ar-C), 123.41 (Ar-C), 55.37 (Aliph-C), 42.35 (Aliph-C). LC/MS 591 $(M + 1)^+$.

*4.1.6.4. 4-Methoxy-N-(2-((4-(6-(3-nitrophenyl)imidazo[2,1-b]thiazol-5-yl)pyrimidin-2-yl)amino)ethyl)benzenesulfonamide (**12d**):*. Yield: 80%. m.p.: 96–9 °C. ^{1}H NMR (400 MHz, DMSO-d_6) δ 8.44 (s, 1H, Ar-H), 8.28 (d, J = 8.0 Hz, 1H, Ar-H), 8.39 (d, J = 5.2 Hz, 1H, Ar-H), 8.08 (d, J = 8.0 Hz, 1H, Ar-H), 7.73 (d, J = 8.8 Hz, 3H, Ar-H), 7.66 (d, J = 8.8 Hz, 2H, Ar-H), 7.52 (s, 1H, Ar-H), 7.08 (t, J = 4.4 Hz, 2H, Ar-H), 6.42 (s, 1H, NH), 3.79 (s, 3H, OCH_3), 3.40 (s, 2H, Aliph-H), 2.94 (d, J = 6.0 Hz, 2H, Aliph-H). ^{13}C NMR (100 MHz, DMSO-d_6) δ 167.63(Ar-C), 167.52 (Ar-C), 148.30 (Ar-C), 136.65 (Ar-C), 135.19 (Ar-C), 132.45 (Ar-C), 132.23(Ar-C), 130.69 (Ar-C), 129.10 (Ar-C), 129.00(Ar-C), 123.22 (Ar-C), 122.53(Ar-C), 114.83 (Ar-C), 114.22(Ar-C), 56.07 (OCH_3), 42.57 (Aliph-C), 42.36 (Aliph-C). LC/MS 553 $(M + 1)^+$.

*4.1.6.5. 4-Chloro-N-(2-((4-(6-(3-nitrophenyl)imidazo[2,1-b]thiazol-5-yl) pyrimidin-2-yl)amino)ethyl)benzenesulfonamide (**12e**):*. Yield: 45%. m.p.: 150–1 °C. ^{1}H NMR (400 MHz, DMSO-d_6) δ 8.44 (s, 1H, Ar-H), 8.28 (d, J = 7.6 Hz, 1H, Ar-H), 8.14 (d, J = 5.2 Hz, 1H, Ar-H), 8.08 (d, J = 8.0 Hz, 1H, Ar-H), 7.81 (d, J = 6.8 Hz, 2H, Ar-H), 7.76 (t, J = 8.0 Hz, 1H, Ar-H), 7.57–7.63 (m, 3H, Ar-H), 7.52 (s, 1H, Ar-H), 6.43 (s, 1H, NH), 3.41 (s, 2H, Aliph-H), 2.97 (d, J = 5.2 Hz, 2H, Aliph-H). LC/MS 557 $(M + 1)^+$.

*4.1.6.6. 4-Bromo-N-(2-((4-(6-(3-nitrophenyl)imidazo[2,1-b]thiazol-5-yl) pyrimidin-2-yl)amino)ethyl)benzenesulfonamide (**12f**):*. Yield: 60%. m.p.: 118–9 °C. ^{1}H NMR (400 MHz, DMSO-d_6) δ 8.44 (s, 1H, Ar-H), 8.28 (d, J = 7.6 Hz, 1H, Ar-H), 8.13 (d, J = 4.8 Hz, 1H, Ar-H), 8.08 (d, J = 8.0 Hz, 1H, Ar-H), 7 (s, 1H, Ar-H), 7.73–7.77 (m, 5H, Ar-H), 7.52 (s, 1H, Ar-H), 6.42 (s, 1H, Ar-H), 3.36 (s, 2H, Aliph-H), 3.00 (t, J = 6.4 Hz, 2H, Aliph-H). ^{13}C NMR (100 MHz, DMSO-d_6) δ 163.12 (Ar-C), 162.98(Ar-H), 148.37 (Ar-C), 140.16 (Ar-C), 136.66 (Ar-C), 132.68 (Ar-C), 130.69 (Ar-C), 128.98 (Ar-C), 126.6 (Ar-C), 123.74 (Ar-C), 119.54 (Ar-C), 114.37 (Ar-C), 114.16 (Ar-C), 49.45 (Aliph-C), 42.31 (Aliph-C). LC/MS 601 $(M + 1)^+$.

*4.1.6.7. 4-Fluoro-N-(2-((4-(6-(3-nitrophenyl)imidazo[2,1-b]thiazol-5-yl) pyrimidin-2-yl)amino)ethyl)benzenesulfonamide (**12 g**):*. Yield: 65%. m.p.: 160–2 °C. ^{1}H NMR (400 MHz, DMSO-d_6) δ 8.44 (s, 1H, Ar-H), 8.28 (d, J = 7.2 Hz, 1H, Ar-H), 8.14 (d, J = 5.2 Hz, 1H, Ar-H), 8.08 (d, J = 8.0 Hz, 1H, Ar-H), 7.85–7.89 (m, 2H, Ar-H), 7.81 (d, J = 6.8 Hz, 1H, Ar-H), 7.76 (d, J = 8.0 Hz, 1H, Ar-H), 7.54–7.61 (m, 1H, Ar-H), 7.52 (s, 1H, NH), 7.38–7.43 (m, 2H, Ar-H), 6.43 (s, 1H, Ar-H), 3.41 (s, 2H, Aliph-H), 2.98 (d, J = 5.2 Hz, 2H, Aliph-H). ^{13}C NMR (100 MHz, DMSO-d_6) δ 163.67 (Ar-C),148.38 (Ar-C), 136.64 (Ar-C), 130.69 (Ar-C), 130.00 (Ar-C), 129.64 (Ar-C), 126.92 (Ar-C), 123.77 (Ar-C), 123.53 (Ar-C), 116.87 (Ar-C), 116.64 (Ar-C), 42.59 (Aliph-C), 42.34 (Aliph-C). LC/MS 541 $(M + 1)^+$.

*4.1.6.8. N-(2-((4-(6-(3-Nitrophenyl)imidazo[2,1-b]thiazol-5-yl) pyrimidin-2-yl)amino)ethyl)naphthalene-1-sulfonamide (**12 h**):*. Yield: 70%. m.p.: 148–9 °C. ^{1}H NMR (400 MHz, DMSO-d_6) δ 8.27 (s, 2H, Ar-H), 8.06 (d, J = 8.4 Hz, 1H, Ar-H), 7.95 (s, 4H, Ar-H), 7.82 (d, J = 8.4 Hz, 1H, Ar-H), 7.74 (d, J = 7.6 Hz, 1H, Ar-H), 7.62 (d, J = 9.2 Hz, 1H, Ar-H), 7.63 (d, J = 8.4 Hz, 3H, Ar-H), 7.51 (s, 1H, Ar-H), 6.33 (s, 1H, Ar-H), 3.39 (s, 2H, Aliph-H), 3.04 (s, 2H, Aliph-H). ^{13}C NMR (100 MHz, DMSO-d_6) δ167.27 (Ar-C), 163.45 (Ar-C), 148.37 (Ar-C), 136.66 (Ar-C), 134.52 (Ar-C), 132.12 (Ar-C), 130.68 (Ar-C), 129.78 (Ar-C), 129.53 (Ar-C), 128.99 (Ar-C), 128.15 (Ar-C), 127.85 (Ar-C), 127.77 (Ar-C), 122.68 (Ar-C), 114.26 (Ar-C), 108.06(Ar-C), 42.58 (Aliph-C), 42.38 (Aliph-C). LC/MS 573 $(M + 1)^+$.

*4.1.6.9. 3-Fluoro-N-(3-((4-(6-(3-nitrophenyl)imidazo[2,1-b]thiazol-5-yl) pyrimidin-2-yl)amino)propyl)benzenesulfonamide (**13a**):*. Yield: 65%.

m.p.: 155–7 °C. ^{1}H NMR (400 MHz, DMSO-d_6) δ 8.44 (s, 1H, Ar-H), 8.27 (d, J = 8.0 Hz, 1H, Ar-H), 8.13 (d, J = 5.2 Hz, 1H, Ar-H), 8.12 (d, J = 7.6 Hz, 1H, Ar-H), 7.76 (q, 2H, Ar-H), 7.64 (s, 2H, Ar-H), 7.58 (d, J = 8.4 Hz, 1H, Ar-H), 7.52 (d, J = 4.6 Hz, 2H, Ar-H), 6.41 (s, 1H, Ar-H), 3.31 (t, J = 6.4 Hz, 2H, Aliph-H), 2.91 (s, 2H, Aliph-H), 1.71 (t, J = 6.8 Hz, 2H, Aliph-H). ^{13}C NMR (100 MHz, DMSO-d_6) δ 163.45 (Ar-C), 162.64 (Ar-C), 160.99 (Ar-C), 151.89 (Ar-C), 148.36 (Ar-C), 143.08 (Ar-C), 136.69 (Ar-C), 135.77 (Ar-C), 132.04 (Ar-C), 130.63 (Ar-C), 123.33 (Ar-C), 120.03 (Ar-C), 119.81 (Ar-C), 113.91 (Ar-C), 41.12 (Aliph-C), 38.7 (Aliph-C), 29.47 (Aliph-C). LC/MS 555 $(M + 1)^+$.

4.1.6.10. 4-Methyl-N-(3-((4-(6-(3-nitrophenyl)imidazo[2,1-b]thiazol-5-yl)pyrimidin-2-yl)amino)propyl)benzenesulfonamide ***(13b)****:*. Yield: 75%. m.p.: 103–5 °C. ^{1}H NMR (400 MHz, DMSO-d_6) δ 8.17 (s, 1H, NH), 8.11 (d, J = 5.2 Hz, 1H, Ar-H), 7.66 (d, J = 7.6 Hz, 2H, Ar-H), 7.55–7.51 (m, 2H, Ar-H), 7.46 (d, J = 8.0 Hz, 1H, Ar-H), 7.41 (d, J = 8.8 Hz, 1H, Ar-H), 7.35 (d, J = 6.8 Hz, 3H, Ar-H), 7.29 (t, J = 8.8 Hz, 1H, Ar-H), 6.41 (d, J = 4.0 Hz, 1H, Ar-H), 3.35 (s, 3H, CH3), 3.31 (d, J = 9.6 Hz, 2H, Aliph-H), 2.83 (t, J = 6.0 Hz, 2H, Aliph-H), 1.69 (t, J = 6.8 Hz, 2H,). ^{13}C NMR (100 MHz, DMSO-d_6) δ 163.699 (Ar-C), 162.56 (Ar-C), 161.27 (Ar-C), 155.63 (Ar-C), 142.94 (Ar-C), 138.03 (Ar-C), 137.60 (Ar-C), 131.05 (Ar-C), 130.97 (Ar-C), 126.953 (Ar-C), 125.79 (Ar-C), 116.34 (Ar-C), 115.89 (Ar-C), 41.09 (Aliph-C), 29.52 (Aliph-C), 21.36 (Aliph-C). LC/MS 551 $(M + 1)^+$.

4.1.6.11. N-(3-((4-(6-(3-Nitrophenyl)imidazo[2,1-b]thiazol-5-yl) pyrimidin-2-yl)amino)propyl)-4-(trifluoromethyl)benzenesulfonamide ***(13c)****:*. Yield: 70%. m.p.: 98–100 °C. ^{1}H NMR (400 MHz, $CDCl_3$) δ 8.57 (s, 1H, Ar-H), 8.46 (s, 1H, Ar-H), 8.27 (d, J = 7.2 Hz, 1H, Ar-H), 8.11 (d, J = 3.2 Hz, 1H, Ar-H), 2.02 (d, J = 6.4 Hz, 1H, Ar-H), 7.95 (d, J = 6.0 Hz, 2H, Ar-H), 7.75 (d, J = 6.8 Hz, 2H, Ar-H), 7.63 (d, J = 7.2 Hz, 1H, Ar-H), 7.04 (s, 1H, Ar-H), 6.48 (s, 1H, Ar-H), 5.54 (s, 1H, NH), 3.61 (d, J = 3.6 Hz, 2H, Aliph-H), 3.14 (s, 2H, Aliph-H), 1.84 (s, 2H, Aliph-H). ^{13}C NMR (100 MHz, $CDCl_3$) δ 162.47 (Ar-C), 157.81 (Ar-C), 156.75 (Ar-C), 152.50 (Ar-C), 148.37 (Ar-C), 146.87 (Ar-C), 144.01 (Ar-C), 136.36 (Ar-C), 135.13 (Ar-C), 129.64 (Ar-C), 127.38 (Ar-C), 126.26 (Ar-C), 124.12 (CF_3), 123.28 (Ar-C), 121.49 (Ar-C), 113.66 (Ar-C), 107.37 (Ar-C), 40.21 (Aliph-C), 38.12 (Aliph-C), 30.1 (Aliph-C). LC/MS 605 $(M + 1)^+$.

4.1.6.12. 4-Methoxy-N-(3-((4-(6-(3-nitrophenyl)imidazo[2,1-b]thiazol-5-yl)pyrimidin-2-yl)amino)propyl)benzenesulfonamide ***(13d)****:*. Yield: 80%. m.p.: 153–5 °C. ^{1}H NMR (400 MHz, $CDCl_3$) δ 8.57 (s, 1H, Ar-H), 8.49 (s, 1H, Ar-H), 8.26 (d, J = 6.4 Hz, 1H, Ar-H), 8.09 (s, 1H, Ar-H), 8.03 (d, J = 6.4 Hz, 1H, Ar-H), 7.77 (s, 2H, Ar-H), 7.63 (s, 1H, Ar-H), 6.93–7.00 (m, 4H, Ar-H), 6.46 (s, 1H, Ar-H), 5.61 (s, 1H, Ar-H), 3.84 (s, 3H, OCH_3), 3.60 (s, 2H, Aliph-C), 3.08 (s, 2H, Aliph-C), 1.84 (s, 2H, Aliph-C). ^{13}C NMR (100 MHz, $CDCl_3$) δ 162.80 (Ar-C), 157.67 (Ar-C), 156.60 (Ar-C), 152.42 (Ar-C), 148.37 (Ar-C), 146.71 (Ar-C), 136.51 (Ar-C), 131.44 (Ar-C), 129.11 (Ar-C), 124.15 (Ar-C), 123.21 (Ar-C), 121.71 (Ar-C), 114.31 (Ar-C), 113.61 (Ar-C), 107.15 (Ar-C), 55.59 (OCH_3), 40.15 (Aliph-C), 38.29 (Aliph-C), 29.79 (Aliph-C). LC/MS 567 $(M + 1)^+$.

4.1.6.13. 4-Chloro-N-(3-((4-(6-(3-nitrophenyl)imidazo[2,1-b]thiazol-5-yl)pyrimidin-2-yl)amino)propyl)benzenesulfonamide ***(13e)****:*. Yield: 75%. m.p.: 100–2 °C. ^{1}H NMR (400 MHz, $CDCl_3$) δ 8.58 (s, 1H, Ar-H), 8.49 (s, 1H, Ar-H), 8.27 (s, 1H, Ar-H), 8.10 (s, 1H, Ar-H), 8.04 (s, 1H, Ar-H), 7.85 (s, 2H, Ar-H), 7.63 (s, 2H, Ar-H), 7.55 (s, 1H, Ar-H), 7.49 (s, 1H, Ar-H), 7.04 (s, 1H, NH), 6.47 (s, 1H, Ar-H), 5.57 (s, 1H, NH), 3.60 (s, 2H, Aliph-H), 3.10 (s, 2H, Aliph-H), 1.85 (s, 2H, Aliph-H). ^{13}C NMR (100 MHz, $CDCl_3$) δ 162.44 (Ar-C), 157.85 (Ar-C), 156.65 (Ar-C), 152.43 (Ar-C), 148.38 (Ar-C), 146.76 (Ar-C), 140.11 (Ar-C), 136.49 (Ar-C), 132.58 (Ar-C), 129.21 (Ar-C), 126.85 (Ar-C), 124.16 (Ar-C), 123.24 (Ar-C), 121.52 (Ar-C), 113.61 (Ar-C), 107.21 (Ar-C), 40.26 (Aliph-C), 38.22 (Aliph-C), 29.93 (Aliph-C). LC/MS 571 $(M + 1)^+$.

4.1.6.14. 4-Bromo-N-(3-((4-(6-(3-nitrophenyl)imidazo[2,1-b]thiazol-5-yl)pyrimidin-2-yl)amino)propyl)benzenesulfonamide ***(13f)****:*. Yield: 70%. m.p.: 105–6 °C. ^{1}H NMR (400 MHz, $CDCl_3$) δ 8.58 (s, 1H, Ar-H), 8.53 (d, J = 4.0 Hz, 1H, Ar-H), 8.33 (d, J = 8.0 Hz, 2H, Ar-H), 8.03 (d, J = 8.0 Hz, 2H, Ar-H), 7.72 (t, J = 8.4 Hz, 3H, Ar-H), 7.63 (d, J = 8.4 Hz, 3H, Ar-H), 7.16 (s, 1H, NH), 6.50 (d, J = 5.6 Hz, 1H, Ar-H), 3.69 (s, 2H, Aliph-H), 3.14 (d, J = 5.2 Hz, 2H, Aliph-H), 1.92 (s, 2H, Aliph-H). ^{13}C NMR (100 MHz, $CDCl_3$) δ 162.33 (Ar-C), 157.65 (Ar-C), 152.51 (Ar-C), 148.38 (Ar-C), 146.91 (Ar-C), 139.27 (Ar-C), 136.41 (Ar-C), 132.42 (Ar-C), 129.65 (Ar-C), 128.42 (Ar-C), 124.15 (Ar-C), 123.29 (Ar-C), 121.44 (Ar-C), 113.71 (Ar-C), 107.26 (Ar-C), 40.22 (Aliph-C), 38.18 (Aliph-C), 29.93 (Aliph-C). LC/MS 616 $(M + 1)^+$.

4.1.6.15. 4-Fluoro-N-(3-((4-(6-(3-nitrophenyl)imidazo[2,1-b]thiazol-5-yl)pyrimidin-2-yl)amino)propyl)benzenesulfonamide ***(13 g)****:*. Yield: 60%. m.p.: 158–160 °C. ^{1}H NMR (400 MHz, $CDCl_3$) δ 8.57 (s, 1H, Ar-H), 8.47 (s, 1H, Ar-H), 8.27 (s, 1H, Ar-H), 8.10 (s, 1H, Ar-H), 8.03 (s, 1H, Ar-H), 7.85 (s, 2H, Ar-H), 7.63 (s, 1H, Ar-H), 7.04–7.30 (m, 3H, Ar-H), 6.47 (s, 1H, Ar-H), 5.59 (s, 1H, NH), 3.59 (s, 2H, Aliph-H), 3.09 (s, 2H, Aliph-H), 1.83 (s, 2H, Aliph-H). ^{13}C NMR (100 MHz, $CDCl_3$) δ 166.21 (Ar-C), 163.68 (Ar-C), 162.44 (Ar-C), 157.81 (Ar-C), 156.67 (Ar-C), 152.44 (Ar-C), 148.36 (Ar-C), 14,678 (Ar-C), 136.35 (Ar-C), 135.17 (Ar-C), 129.59 (Ar-C), 124.14 (Ar-C), 121.45 (Ar-C), 116.33 (Ar-C), 113.62 (Ar-C), 107.25 (Ar-C), 40.23 (Aliph-C), 38.19 (Aliph-C), 29.91 (Aliph-C). LC/MS 555 $(M + 1)^+$.

4.1.6.16. N-(3-((4-(6-(3-Nitrophenyl)imidazo[2,1-b]thiazol-5-yl) pyrimidin-2-yl)amino)propyl)naphthalene-1-sulfonamide ***(13 h)****:*. Yield: 80%. m.p.: 95–7 °C. ^{1}H NMR (400 MHz, $CDCl_3$) δ 8.52 (s, 1H, Ar-H), 8.40 (d, J = 8.6 Hz, 2H, Ar-H), 8.23 (d, J = 5.2 Hz, 1H, Ar-H), 7.87–8.01 (m, 4H, Ar-H), 7.49–7.71 (m, 3H, Ar-H), 7.28–7.36 (m, 1H, Ar-H), 7.00 (s, 1H, Ar-H), 6.40 (s, 1H, Ar-H), 5.72 (s, 1H, Ar-H), 3.58 (s, 2H, Aliph-H), 3.13 (s, 2H, Aliph-H), 1.83 (s, 2H, Aliph-H). ^{13}C NMR (100 MHz, $CDCl_3$) δ 162.38 (Ar-C), 157.77 (Ar-C), 156.52 (Ar-C), 152.38 (Ar-C), 148.32 (Ar-C), 146.64 (Ar-C), 136.62 (Ar-C), 134.67 (Ar-C), 132.08 (Ar-C), 129.48 (Ar-C), 127.67 (Ar-C), 124.11 (Ar-C), 123.18 (Ar-C), 122.11 (Ar-C), 121.71 (Ar-C), 113.56 (Ar-C), 107.05 (Ar-C), 40.40 (Aliph-C), 38.27 (Aliph-C), 29.81 (Aliph-C). LC/MS 587 $(M + 1)^+$.

4.2. Biological evaluation

4.2.1. In vitro enzyme assay

Reaction Biology Corp. Kinase HotSpotSM service was used for screening of final compounds. Assay protocol: as reported on Reaction Biology Corp. website using 1 μM concentration of ATP [35]. Isolated human BRAF (V599E) was used and MEK1 was used as substrate at 1 uM concentration and 1uM ATP concentration (^{33}P labeled ATP was used to produce ^{33}P-Substrate which was a measure for enzyme activity).

4.2.2. In vitro cytotoxicity

Screening against the cancer cell lines was carried out for compounds **12a-h** and **13a-h** at the National Cancer Institute (NCI), Bethesda, Maryland, USA, applying the standard protocol of the NCI. In addition, **13a-h** were evaluated for their antiproliferative activity against melanoma cell lines (A375) using MTT (3-(4,5-dimethylthiazol-2-yl)-2,5-diphenyltetrazolium bromide) assay [33].

4.3. Molecular docking

The X-ray structure of mutated B-Raf (B-Raf V600E) with PLX3203 (native ligand) was downloaded from the protein databank RCSB PDB (PDB ID: 4FK3) [34,36]. The X-ray structure of B-Raf V600E was visualized and manipulated by MOE 2014.13 (Molecular Operating Environment) [37]. The PDB file consist of one domain in form of five

chains; two chains of amino acid residues belonging to the mutated B-Raf, one ligand (PLX3203, PDB ID: 325) and two chains of water molecules of crystallization.

4.3.1. Preparing the B-Raf protein structure for molecular docking

The PDB file was visualized by MOE 2014.13. Both nonbinding amino acid chain and water molecules were removed leaving only the native ligand atoms (PLX2303, PDB ID: 325) and protein amino acid residues. The hydrogen atoms were placed and the overall lowest potential configuration energy was determined and identified. Both ligand and the active site pocket were isolated and visualized through molecular surface tool.

4.3.2. Validation of docking protocol of native ligand with the active site

Native ligand (PLX2303, PDB ID: 325) was considered in the validation of docking process with the active site of phosphodiesterase enzyme. The Rigid Protein Docking protocol was used in the validation step. Triangle Matcher method (bond rotation method) was used in order to generate the native ligand conformations. The produced conformations were ranked with the London dG scoring function. The minimization of conformations energies was accomplished with Forcefield functional form. The identified conformations were rescored with GBVI/WSA dG binding free energy calculation (S, kcal/mol).

4.3.3. Docking of target compounds

Target compounds (**12a-h** and **13a-h**) database were selected as ligand atoms in the molecular docking procedure using the same setting for the native (PLX2303, PDB ID: 325).

4.3.4. Analyzing the docking results

The best conformations of tested compounds (lowest binding score and RMSD values) were selected to be visualized in the B-Raf V600E active site pocket. The 2D interaction of each conformation was pictured to order to identify the binding modes with the possible interactions.

Acknowledgments

This work was supported by Korea Institute of Science and Technology (KIST), and KIST Project (2E29340). We are grateful to the National Cancer Institute (NCI), Bethesda, Maryland, USA, for testing the antiproliferative activity of the target compounds against 60 cancer cell lines of nine different cancer types.

Conflict of interest

The authors declare no conflict of interest.

Appendix A. Supplementary data

Supplementary data to this article can be found online at https://doi.org/10.1016/j.bioorg.2020.103967.

References

[1] K.G. Krishnan, C.U. Kumar, W.-M. Lim, C.-W. Mai, P.V. Thanikachalam, C. Ramalingan, Novel cyanoacetamide integrated phenothiazines: Synthesis, characterization, computational studies and in vitro antioxidant and anticancer evaluations, J. Mol. Struct. 1199 (2020) 127037.
[2] L.H. Amin, T.Z. Shawer, A.M. El-Naggar, H.M. El-Sehrawi, Design, synthesis, anticancer evaluation and docking studies of new pyrimidine derivatives as potent thymidylate synthase inhibitors, Bioorg. Chem. 91 (2019) 103159.
[3] G.L. Patrick, An introduction to medicinal chemistry, Oxford University Press, 2013.
[4] M.S. Abdel-Maksoud, U.M. Ammar, M.I. El-Gamal, M.M.G. El-Din, K.I. Mersal, E.M. Ali, K.H. Yoo, K.-T. Lee, C.-H. Oh, Design, synthesis, and anticancer activity of imidazo [2, 1-b] oxazole-based RAF kinase inhibitors, Bioorg. Chem. 93 (2019) 103349.
[5] F. Ahmad, N. Avabhrath, S. Natarajan, J. Parikh, K. Patole, B.R. Das, Molecular evaluation of BRAF V600 mutation and its association with clinicopathological characteristics: First findings from Indian malignant melanoma patients, Cancer genetics 231 (2019) 46–53.
[6] V.K. Goel, A.J. Lazar, C.L. Warneke, M.S. Redston, F.G. Haluska, Examination of mutations in BRAF, NRAS, and PTEN in primary cutaneous melanoma, J, Invest. Dermatol. 126 (2006) 154–160.
[7] A. Gorden, I. Osman, W. Gai, D. He, W. Huang, A. Davidson, A.N. Houghton, K. Busam, D. Polsky, Analysis of BRAF and N-RAS mutations in metastatic melanoma tissues, Cancer Res. 63 (2003) 3955–3957.
[8] C. Willmore-Payne, J.A. Holden, S. Tripp, L.J. Layfield, Human malignant melanoma: detection of BRAF-and c-kit–activating mutations by high-resolution amplicon melting analysis, Hum. Pathol. 36 (2005) 486–493.
[9] T. Shibata, A. Kokubu, M. Miyamoto, Y. Sasajima, N. Yamazaki, Mutant IDH1 confers an in vivo growth in a melanoma cell line with BRAF mutation, The American journal of pathology 178 (2011) 1395–1402.
[10] F. Janku, J.J. Lee, A.M. Tsimberidou, D.S. Hong, A. Naing, G.S. Falchook, S. Fu, R. Luthra, I. Garrido-Laguna, R. Kurzrock, PIK3CA mutations frequently coexist with RAS and BRAF mutations in patients with advanced cancers, PLoS ONE 6 (2011) e22769.
[11] H. Davies, G.R. Bignell, C. Cox, P. Stephens, S. Edkins, S. Clegg, J. Teague, H. Woffendin, M.J. Garnett, W. Bottomley, Mutations of the BRAF gene in human cancer, Nature 417 (2002) 949.
[12] U.M. Ammar, M.S. Abdel-Maksoud, C.-H. Oh, Recent advances of RAF (rapidly accelerated fibrosarcoma) inhibitors as anti-cancer agents, Eur. J. Med. Chem. 158 (2018) 144–166.
[13] M. Libra, G. Malaponte, P.M. Navolanic, P. Gangemi, V. Bevelacqua, L. Proietti, B. Bruni, F. Stivala, M.C. Mazzarino, S. Travali, Analysis of BRAF mutation in primary and metastatic melanoma, Cell Cycle 4 (2005) 1382–1384.
[14] W. Liu, J.W. Kelly, M. Trivett, W.K. Murray, J.P. Dowling, R. Wolfe, G. Mason, J. Magee, C. Angel, A. Dobrovic, Distinct clinical and pathological features are associated with the BRAFT1799A (V600E) mutation in primary melanoma, J, Invest. Dermatol. 127 (2007) 900–905.
[15] B.S. Hoyt, S. Yan, K.D. Linos, S. Momtahen, A. Sriharan, T.-A.N. Tran, G.J. Tsongalis, R.R. O'Meara, D.C. Green, R.E. LeBlanc, BRAF V600E mutations are not an oncogenic driver of solitary xanthogranuloma and reticulohistiocytoma: Testing may be useful in screening for Erdheim-Chester disease, Exp. Mol. Pathol. 104320 (2019).
[16] C. Peyssonnaux, A. Eychène, The Raf/MEK/ERK pathway: new concepts of activation, Biol. Cell 93 (2001) 53–62.
[17] K. Amin, O. El-Badry, D.A. Rahman, U. Ammar, Synthesis and In Vitro Biological Evaluation of New Pyrido [2, 3-b] pyrazinone-Based Cytotoxic Agents and Molecular Docking as BRAF Inhibitors, ChemistrySelect 4 (2019) 8882–8885.
[18] J.-J. Liu, H. Zhang, J. Sun, Z.-C. Wang, Y.-S. Yang, D.-D. Li, F. Zhang, H.-B. Gong, H.-L. Zhu, Synthesis, biological evaluation of novel 4, 5-dihydro-2H-pyrazole 2-hydroxyphenyl derivatives as BRAF inhibitors, Bioorg. Med. Chem. 20 (2012) 6089–6096.
[19] A. Scholtens, M.G. Foppen, C. Blank, J. van Thienen, H. Van Tinteren, J. Haanen, Vemurafenib for BRAF V600 mutated advanced melanoma: results of treatment beyond progression, Eur. J. Cancer 51 (2015) 642–652.
[20] E. Funck-Brentano, J. Alvarez, C. Longvert, E. Abe, A. Beauchet, C. Funck-Brentano, P. Saiag, Plasma vemurafenib concentrations in advanced BRAFV600mut melanoma patients: impact on tumour response and tolerance, Ann. Oncol. 26 (2015) 1470–1475.
[21] G.T. Gibney, J.S. Zager, Clinical development of dabrafenib in BRAF mutant melanoma and other malignancies, Expert Opin. Drug Metab. Toxicol. 9 (2013) 893–899.
[22] Z. Li, K. Jiang, X. Zhu, G. Lin, F. Song, Y. Zhao, Y. Piao, J. Liu, W. Cheng, X. Bi, Encorafenib (LGX818), a potent BRAF inhibitor, induces senescence accompanied by autophagy in BRAFV600E melanoma cells, Cancer Lett. 370 (2016) 332–344.
[23] P. Koelblinger, O. Thuerigen, R. Dummer, Development of encorafenib for BRAF-mutated advanced melanoma, Curr. Opin. Oncol. 30 (2018) 125.
[24] E.M. Ali, M.S. Abdel-Maksoud, C.-H. Oh, Thieno [2, 3-d] pyrimidine as a promising scaffold in medicinal chemistry: Recent advances, Bioorg. Med. Chem. (2019).
[25] B. Kuhn, P. Mohr, M. Stahl, Intramolecular hydrogen bonding in medicinal chemistry, J. Med. Chem. 53 (2010) 2601–2611.
[26] A. Alex, D.S. Millan, M. Perez, F. Wakenhut, G.A. Whitlock, Intramolecular hydrogen bonding to improve membrane permeability and absorption in beyond rule of five chemical space, MedChemComm 2 (2011) 669–674.
[27] V.K. Vyas, G. Qureshi, D. Oza, H. Patel, K. Parmar, P. Patel, M.D. Ghate, Synthesis of 2-, 4,-6-, and/or 7-substituted quinoline derivatives as human dihydroorotate dehydrogenase (hDHODH) inhibitors and anticancer agents: 3D QSAR-assisted design, Bioorg. Med. Chem. Lett. 29 (2019) 917–922.
[28] P. Baumann, S. Mandl-Weber, A. Völkl, C. Adam, I. Bumeder, F. Oduncu, R. Schmidmaier, Dihydroorotate dehydrogenase inhibitor A771726 (leflunomide) induces apoptosis and diminishes proliferation of multiple myeloma cells, Mol. Cancer Ther. 8 (2009) 366–375.
[29] M.S. Abdel-Maksoud, U.M. Ammar, C.-H. Oh, Anticancer profile of newly synthesized BRAF inhibitors possess 5-(pyrimidin-4-yl) imidazo [2, 1-b] thiazole scaffold, Bioorg. Med. Chem. 27 (2019) 2041–2051.
[30] M.S. Abdel-Maksoud, M.-R. Kim, M.I. El-Gamal, M.M.G. El-Din, J. Tae, H.S. Choi, K.-T. Lee, K.H. Yoo, C.-H. Oh, Design, synthesis, in vitro antiproliferative evaluation, and kinase inhibitory effects of a new series of imidazo [2, 1-b] thiazole

derivatives, Eur. J. Med. Chem. 95 (2015) 453–463.
[31] R.F. Heck, Palladium-catalyzed vinylation of organic halides, Org. React. 27 (2004) 345–390.
[32] S.L. Holbeck, J.M. Collins, J.H. Doroshow, Analysis of food and drug administration–approved anticancer agents in the NCI60 panel of human tumor cell lines, Mol Cancer Ther 9 (2010) 1451–1460.
[33] T. Mosmann, Rapid colorimetric assay for cellular growth and survival: application to proliferation and cytotoxicity assays, J. Immunol. Methods 65 (1983) 55–63.
[34] J. Tsai, J.T. Lee, W. Wang, J. Zhang, H. Cho, S. Mamo, R. Bremer, S. Gillette, J. Kong, N.K. Haass, Discovery of a selective inhibitor of oncogenic B-Raf kinase with potent antimelanoma activity, Proc. Natl. Acad. Sci. 105 (2008) 3041–3046.
[35] Reaction Biology Corp. (RBC); http://www.reactionbiology.com.
[36] RCSB Protein Data Bank; https://www.rcsb.org/structure/4fk3.
[37] Molecular Operating Environment (MOE) 2014.13; https://www.chemcomp.com/.